ACS APPLIED MATERIALS & INTERFACES

Research Article

www.acsami.org

A Surface-Enhanced Raman Scattering Optrode Prepared by *in Situ* Photoinduced Reactions and Its Application for Highly Sensitive On-Chip Detection

Shaoyan Wang,[†] Chunyu Liu,[†] Hailong Wang,[†] Gang Chen,[†] Ming Cong,[†] Wei Song,[†] Qiong Jia,[‡] Shuping Xu,*[,†] and Weiqing Xu[†]

[†]State Key Laboratory of Supramolecular Structure and Materials, Institute of Theoretical Chemistry, Jilin University, 2699 Qianjin Avenue, Changchun 130012, China

[‡]Chemical Sciences of Jilin University, 2699 Qianjin Avenue, Changchun 130012, China

ABSTRACT: A surface-enhanced Raman scattering (SERS)-active optical fiber sensor combining the optical fiber waveguide with various SERS substrates has been a powerful analytical tool for *in situ* and long-distance SERS detection with high sensitivity. The design and modification of a high-quality SERS-active sensing layer are important topics in the development of novel SERS-active optical fiber sensors. Here, we prepared a highly sensitive SERS-active optrode by *in situ* fabrication of a three-dimensional porous structure on the optical fiber end via a photoinduced polymerization reaction, followed by the growth of photochemical silver nanoparticles above the porous polymer material. The fabrication process is rapid (finished within 1 h) and can be on line under light control. The porous structure supports vast silver nanoparticles, which allows for strong electromagnetic enhancement of SERS. Interestingly, the preparation of this SERS optrode and its utilization for SERS detection can all be conducted in a microfluidic chip. The qualitative and quantitative on-chip SERS sensing of organic pollutants and pesticides has been achieved by this SERS optrode-integrated microfluidic chip, and its high detection sensitivity makes it a promising factor in the analysis of liquid systems.

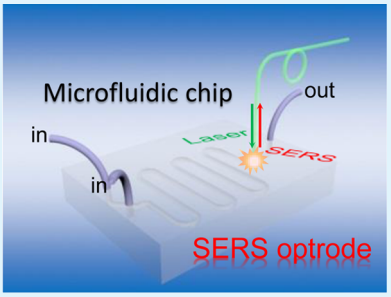

KEYWORDS: *SERS, porous structure, photoinduced growth, on-chip detection, microfluidic chip*

1. INTRODUCTION

A surface-enhanced Raman scattering (SERS) technique increases the intensity of the weak Raman signal 1 million-fold when the probed molecules are adsorbed on the nanoscale roughness metal surface.[1] Enormous signal enhancement permits an ultrahigh detection sensitivity for analytes and extends SERS applications to broader fields, such as explosive substance detection,[2] pesticide residue inspection,[3] toxin tracing,[4] etc. Moreover, SERS is a powerful analytical tool with respect to fingerprint information, which makes it possible to track analytes with individual identities in a complicated system. Many advantages of SERS have attracted a great number of researchers in diversified fields, and their efforts have been devoted to allowing the SERS technique to become an interdisciplinary subject.

One of these attempts is to combine a SERS technique with an optical waveguide to produce optically integrated devices. In these designs, a SERS-active sensing layer usually consisting of metal nanoparticles or a metal film is required to fix on the optical elements. The optical waveguide plays multiple roles in incident light guiding and Raman scattering light collection. Many features of the optical waveguide components can be employed to improve the light coupling efficiency in SERS excitation and emission.[5] One of the important optical waveguide components, the optical fiber, has many advantages, such as low signal loss and little external interference. Optical fiber sensors decorated with SERS-sensing layers have been well designed and used for long-distance, on-line, *in situ*, and *in vivo* monitoring.[6−18] The methods of fabrications for SERS-active sensing layers on the optical fiber tips include vacuum evaporation deposition of metal,[10] high-pressure chemical deposition of metal,[11] assembly of metal colloidal nanoparticles (NPs),[12−14] laser-induced metal deposition,[15−18] etc. To obtain a high SERS enhancement activity in a SERS optical sensor, the geometry of the metal plays a key role due in the physical enhancement mechanism of SERS.[19,20] The high loading and the proper aggregation of metal nanoparticles are favorable for a strong SERS signal.[20−24]

In the design presented here, we developed a SERS optrode, which has a three-dimensional (3D) pore structure on an optical fiber tip, decorated with a large loading of metal nanoparticles. The 3D pore structure was prepared by the *in situ* light polymerization of glycidyl methacrylate (GMA) and 2,2′-dimethoxy-2-phenylacetophenone (DMPA), and then silver nanoparticles were grown *in situ* on the 3D porous polymer. We designed a dual Y-type light path for both the fabrication of this SERS optrode and its SERS measurement. In this manner, two light-induced processes requiring different

Received: April 23, 2014
Accepted: June 30, 2014
Published: June 30, 2014

Scheme 1. Pretreatment of the Terminal End of an Optical Fiber and the Preparation of a Complex SERS-Active Sensing Layer on It

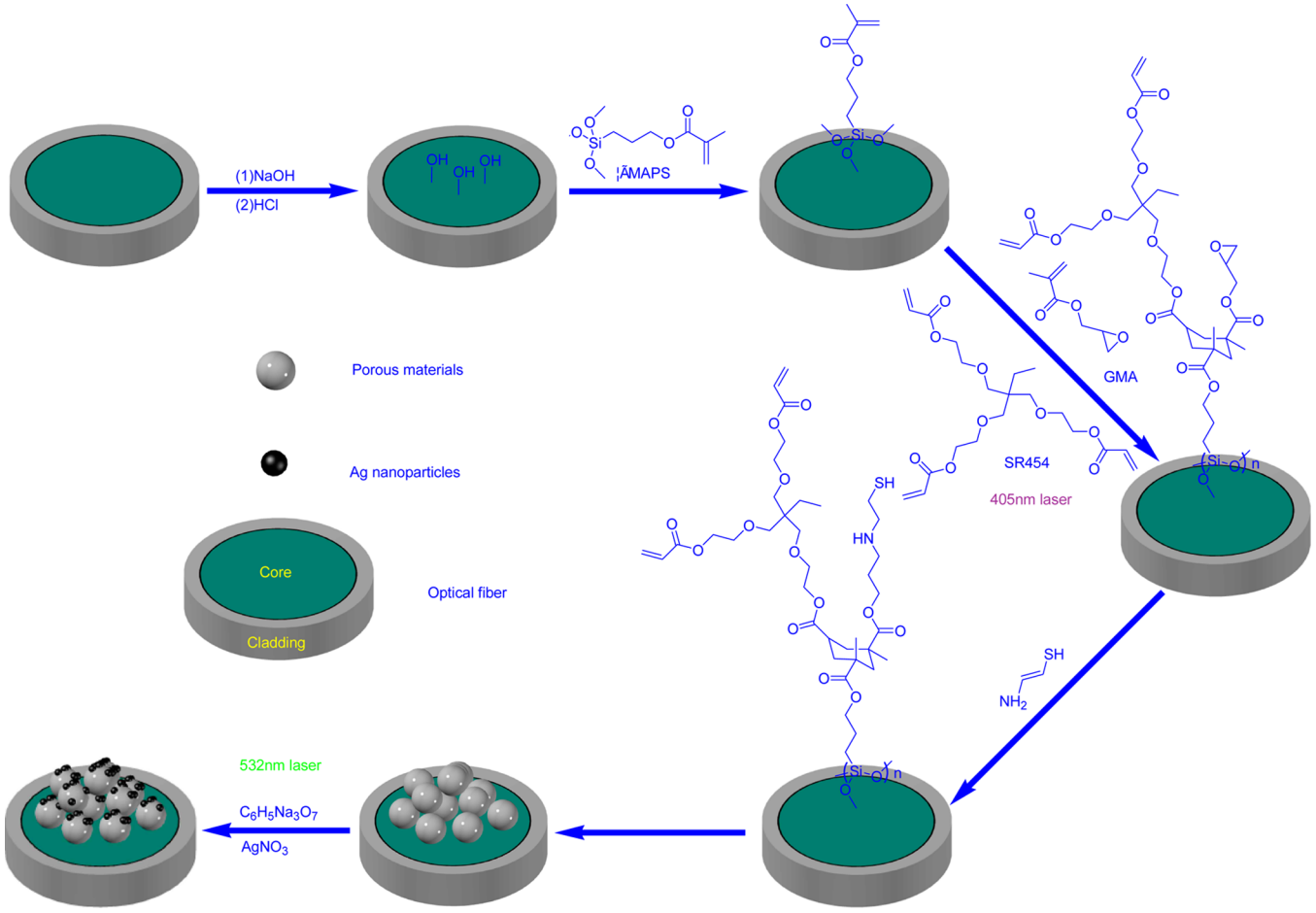

lasers (405 and 532 nm) can be conducted sequentially, and the collection of the SERS signal under the 532 nm laser can be achieved via the same optical fiber. Because the growth of the SERS-sensing layer on the fiber end is totally under light control, this SERS optrode can be constructed *in situ* in the microfluidic channel. This SERS optrode-integrated microfluidic system achieved the on-chip SERS sensing of many analytes, even a pH response. This SERS optrode exhibited very strong SERS activity and high detection sensitivity.

2. EXPERIMENTAL SECTION

2.1. Materials. Glycidyl methacrylate (GMA) and 2,2′-dimethoxy-2-phenylacetophenone (DMPA) were purchased from Aladdin Co., Ltd. Ethoxylated trimethylolpropane triacrylate (SR454), 3-(trimethoxysilyl)propyl methacrylate (r-MAPS), cysteamine, and 4-mercaptopyridine (4-Mpy, 95%) were purchased from Sigma-Aldrich Co., Ltd. Thiram (97%) was obtained from Aladdin. All other agents were obtained from Beijing Chemical Industry. All the chemicals were used without further purification. Ultrapure water was prepared with an ultrapure water purification system (18.1 MΩ). Microfluidic channels were engraved with an engraving machine on a poly(methyl methacrylate) (PMMA) mass (purphased from Foshan City Shunde Jundao Optical Sheet Manufacturing Co., Ltd.). Teflon tape was purchased from Tianjin Tiansu Science & Technology Group Co., Ltd.

2.2. Pretreatment of an Optical Fiber. Multimodal quartz optical fibers used in the experiments have a cladding of 15 μm and a core of 400 μm with a numerical aperture (NA) of 0.37, which was purchased from Nanjing Chunhui Science and Technology Industrial Co., Ltd. Optical fibers were cut into 20 cm pieces that needed to be polished and pretreated. First, both ends of an optical fiber were ground with 3000 mesh emery paper for 5 min, 3 μm fiber abrasive sheets for 5 min, and 1 μm fiber abrasive sheets for 5 min. After being polished, they were cleaned with ultrapure water, ethanol, and ultrapure water for a 10 min ultrasonic treatment and dried in air. To activate the surface of an optical fiber, one tip of the cleaned optical fiber (terminal end) was immersed in NaOH (0.1 M), HCl (0.1 M), ultrapure water, and methanol each for 30 min sequentially and then dried. After this, the optical fiber surface has been modified by hydroxide groups, as shown in Scheme 1. Then, we enrich the surface with silyl groups by immersing the optical fiber tip in a 50% (v/v) r-MAPS/methanol solution to bind the functional monomer and cross-linker onto the optical fiber with covalent bonds. Silylation was conducted in a water bath at 45 °C for 12 h. The resulting optical fiber was thoroughly rinsed with methanol before being used.

2.3. Preparation of a SERS-Active Sensing Layer. The fabrication of the complex SERS-active sensing layer involves two steps: porous structure construction and Ag nanoparticle deposition. First, we fabricated a 3D porous polymer structure on the terminal of an optical fiber via an UV light-induced free radical polymerization process.[25−28] Scheme 2a shows the experimental setup for preparing the SERS optrode and how to integrate it with a microfluidic chip. Scheme 2b shows a photo of this setup. Two Y-shape couplers were used to integrate the 405 nm excitation light path for polymerization and the 532 nm laser excitation for inducing Ag deposition and SERS detection. A 405 nm laser with a light power attenuator was employed to photochemically synthesize the porous polymer. The polymerization reaction solution consists of a homogeneous solution of 24% (w/w) GMA (functional monomer), 16% (w/w) SR454 (cross-linker), 50% (w/w) cyclohexanol, 10% (w/w) methanol (porogens),

Scheme 2. Setup for Preparing the SERS-Sensing Layer on an Optical Fiber and Its Pathway for SERS Measurement[a]

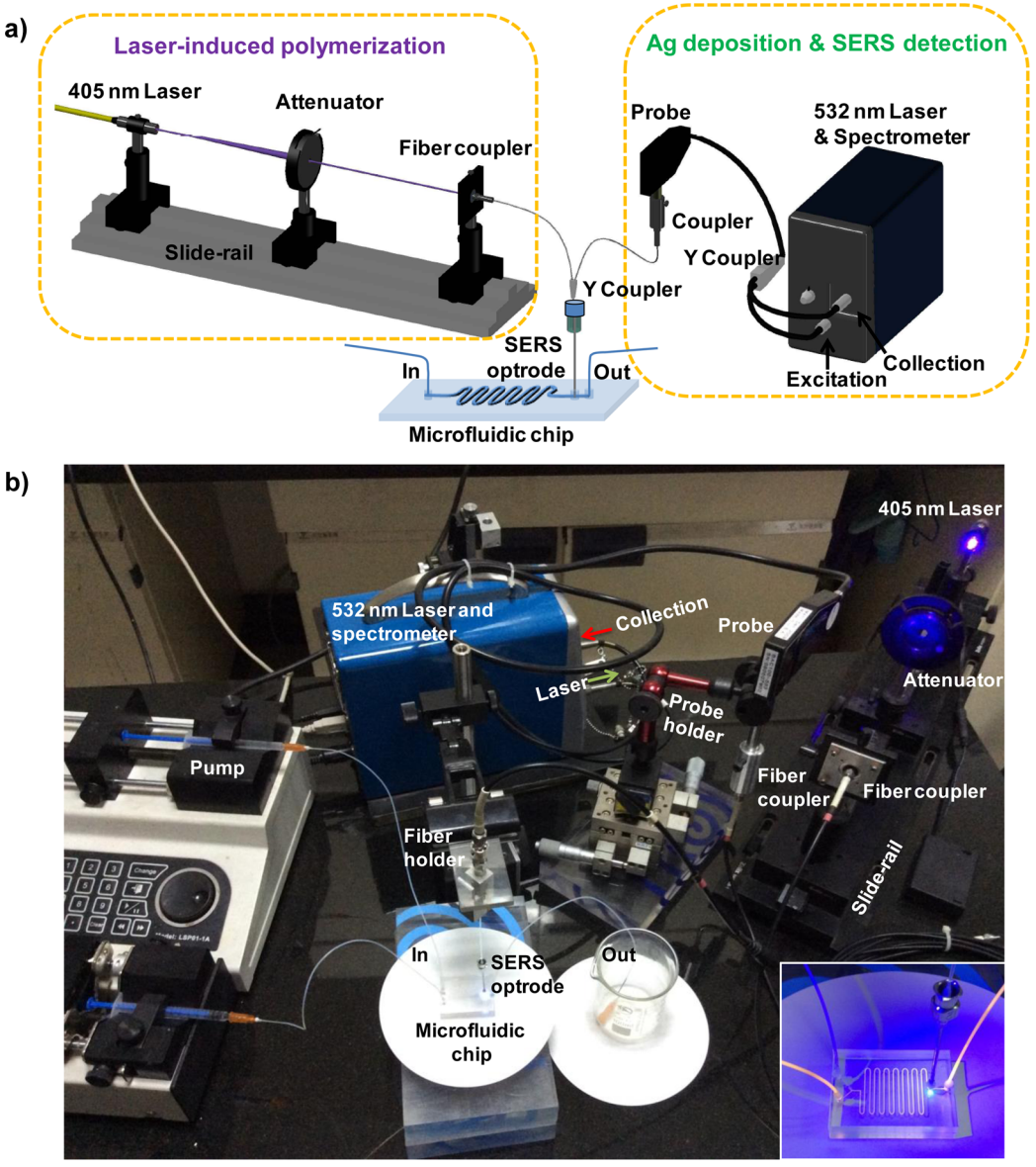

[a]The inset shows an enlarged image of the SERS optrode-integrated microfluidic chip upon measurement of a Rhodanmine 6G solution.

and 1% (w/w) DMPA (with respect to monomers, photoinitiator). We pumped the reaction solution into the microfluidic channel while the terminal end of optical fibers was irradiated with the 405 nm laser. The laser intensity reaching the terminal end was 90 mW cm^{-2} (measured with a COHERENT laser power meter, LM-2 VIS, which was placed toward the terminal end). Free radical initiators decomposed under light induction and made the growing polymers that precipitated from the reaction mixture, forming nuclei. The polymerization then continued both within the swollen nuclei and in the remaining solution. A great number of microspheres were formed, and they were interconnected with each other by polymer chains. The polymerization reaction proceeded for several minutes, and a layer of porous polymer was deposited on the fiber tip (Scheme 1). The laser intensity at the terminal end was monitored, which showed a decreased trend with the formation of the porous polymer (Figure 1). Then, the optical fiber tip was washed with methanol and ultrapure water to remove unreacted components. The morphology of the produced porous polymer was characterized with a scanning electron microscope (SEM, Hitachi New generation Cold Field Emission SEM SU8000 Series, acceleration voltage of 5.0 kV). Nano Measurer version

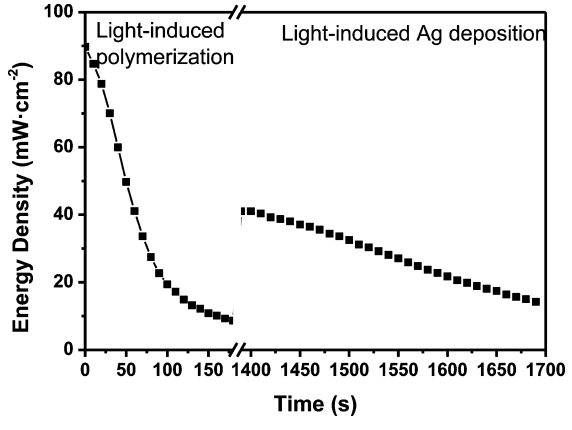

Figure 1. Decay of the laser intensity at the terminal end with the time of light-induced polymerization under a 405 nm laser and Ag deposition under a 532 nm laser.

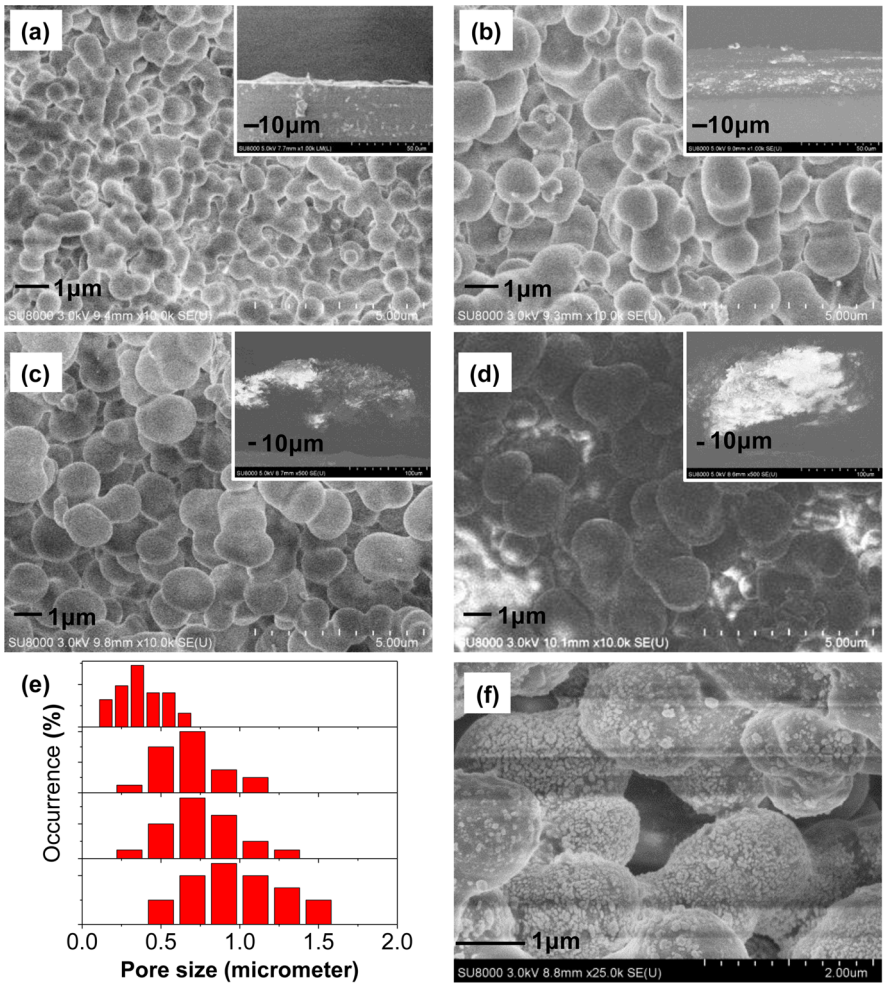

Figure 2. (a–d) SEM images of the poly(GMA-*co*-SR454) porous polymers on the terminal end of optical fibers prepared with different laser polymerization times (1, 2, 3, and 4 min, respectively) under a 90 mW cm^{-2} laser intensity. Insets are the side views of deposited polymers. (e) Statistical results of pore sizes from panels a–d. (f) SEM image of Ag nanoparticles deposited on the porous polymers.

1.2 was used for measuring the pore size distribution. We selected 40 positions (pore size) on each SEM image to give an average pore size.

To deposit silver on the polymer surface, the terminal end with the porous polymer was decorated with cysteamine (2.5 mol/L, 30 min). Next, we *in situ* deposited Ag NPs on the porous polymer structure following a previously reported process.[15,16] This time, a 532 nm laser attached to a miniature (BWTek) Raman spectrometer (BTR-111) was used (see Scheme 2). The terminal end was immersed in the silver growth solution [1:1 (v/v) silver nitrate/trisodium citrate, 1.0×10^{-2} M], which was subjected to 532 nm laser irradiation for 5 min. After that, the SERS optrode was created and cleaned with water before being used.

2.4. SERS Measurement Using SERS Optrodes. To measure SERS spectra of analytes, different concentrations of probing solutions were pumped into the microfluidic channel while its terminal end was immersed in probing solutions and the excitation laser was propagated from other end. The Raman signals were collected by the optical fiber, propagated to the other end, and finally reached the spectrometer.

For comparison, we fabricated another SERS optrode, which consisted of deposited Ag NPs via 532 nm laser irradiation of the naked optical fiber. The details are as follows. One end of the fiber tip was immersed in the growth solution in the channel of the microfluidic chip, and then the laser beam was introduced into the optical fiber core. It should be noted that the laser power spread out of the fiber tip and the laser-induced growth time were both kept the same as those used in the fabrication of the 3D porous SERS optrode. As the modification process reached completion, the microfluidic chip was carefully rinsed with deionized water to remove the physically adsorbed Ag nanoparticles on the optrode.

All SERS spectral data were baselined using Origin version 8, during which 10 number points were chosen to create the baseline by the adjacent-averaging method, and then the baseline was subtracted.

2.5. pH Response Using the SERS Optrode in the Microfluidic Chip. The pH response was achieved on a 4-Mpy-modified SERS optrode. 4-Mpy is sensitive to pH because the structure of 4-Mpy adsorbed on silver surfaces can easily be altered through a protonation or deprotonation reaction occurring on the N atom of the pyridine ring.[29] We first linked 4-Mpy on the SERS optrode by injecting a 4-Mpy aqueous solution (1.0×10^{-3} M) into the microfluidic channel. The mercapto group of 4-Mpy can react with Ag, and it will be linked to Ag by a chemical S–Ag bond. Then, the pH buffers with different concentrations were injected one by one at a flow rate of 5 μL/min. At the same time, the Raman spectra of 4-Mpy at different pH values were *in situ* recorded through the SERS optrode.

3. RESULTS AND DISCUSSION

Because the surface area of a porous structure results in the loadings of metal nanoparticles and analytes, we first optimize the pore size of the porous polymer by its SERS behavior. The pore structure of poly(GMA-*co*-SR454) is affected by many factors, such as the polymerization reaction time, temperature, the ratio of reaction solutions, etc.[30−34] Here, we adopted a light-induced GMA polymerization reaction. Therefore, the

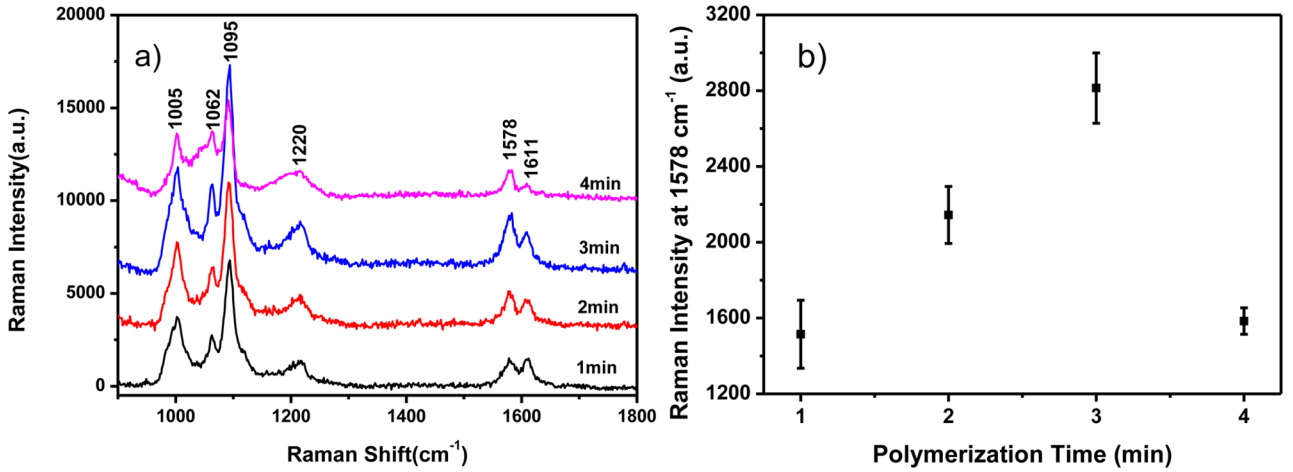

Figure 3. (a) SERS spectra of 4-Mpy (1.0×10^{-4} M) obtained by using different SERS optrodes with different polymer pore sizes fabricated with different polymerization times (1−4 min). The Ag deposition time was 5 min for each trial. (b) SERS intensity of 4-Mpy at 1578 cm^{-1} vs polymerization time. An integration time of 5 s and an accumulation time of 1 were used to record spectra shown in panel a.

irradiation time was tuned and strongly affects the polymerization process, causing the changes in pore size and thickness.

We first measured the laser intensity decay at the terminal end because the growing poly(GMA-*co*-SR454) layer and the next Ag deposition both weaken the transmittance of lasers. Figure 1 displays the monitoring of laser intensity spilled out of the terminal end with the polymerization and Ag deposition time. It can be found that the laser intensity decayed suddenly to 5.6 mW cm^{-2}. The formed poly(GMA-*co*-SR454) layer is opaque for 405 nm light. Then, we turned off the 405 nm laser and removed the unreacted monomers and unabsorbed polymer by pumping methanol. In the following light-induced Ag deposition process, a 532 nm laser was used and the laser intensity reaching the terminal end was ∼41.2 mW cm^{-2}. The transmittance continued to decay. After a 5 min Ag deposition, a SERS-sensing layer was formed on the terminal end of an optical fiber. The total fabrication time was 28 min, which is fast and totally under light control.

Figure 2 shows the SEM images of polymer pore sizes fabricated with different polymerization times. The pore size distributions (Figure 2e) show average pore sizes of 0.38, 0.70, 0.76, and 0.98 μm for polymerization times of 1, 2, 3, and 4 min, respectively, the sizes increasing with an increasing polymerization time. The average thicknesses are 4.5, 31.0, 98.1, and 148.5 μm for panels a−d of Figure 2, respectively.

As we can expect, overly thin and overly thick polymer layers are both negative to the high SERS signal. A very thin polymer layer would supply a limited surface area, causing fewer Ag NPs and a small contribution to SERS enhancement. An overly thick polymer layer would lead to a large light loss, blocking the excited light from arriving in the Ag NPs and also forbidding SERS signal collection. To explore the pore size and thickness effect of 3D porous polymers, SERS spectra of probe molecules on different pore size polymer structures with Ag NP deposition were recorded. Figure 2f shows the morphology of the poly(GMA-*co*-EDMA) porous polymer after Ag NP deposition. It is found that there were a great number of Ag NPs formed on the surface of polymer particles, and the Ag NPs yielded a certain level of aggregation. Figure 3 shows the SERS spectra with different polymerization times. The highest SERS can be observed when the polymerization time is 3 min, corresponding to a polymer pore size of 0.76 μm and a thickness of ∼98 μm. This optimization is based on the consideration of the loading of Ag NPs. We think it is a more important factor in this case than the localized electromagnetic field distribution that is a nanoscopic interpretation of SERS enhancement in many other studies. Because of the results shown in Figure 3, we used the porous polymer synthesized with a polymerization time of 3 min for further SERS detection.

We also compared the SERS behaviors of SERS optrodes with or without 3D porous structure. A SERS optrode constructed by depositing Ag directly on the optical fiber tip via a light-induced growth method was used for SERS measurements. Figure 4 displays the SEM image of the SERS

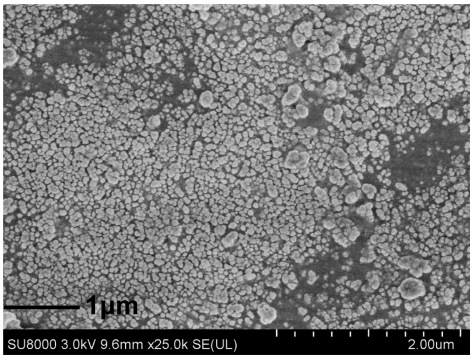

Figure 4. SEM image of the SERS optrode prepared by laser-induced Ag NP deposition.

optrode tip only with Ag NP deposition. It can be found that the deposited Ag particle size on the optical fiber (91 ± 4 nm) is almost the same as that on the 3D porous polymer-decorated optical fiber (89 ± 3 nm). Figure 5 displays a comparison of SERS results achieved from two SERS optrodes when they were probed with a 4-Mpy solution. The intensity of the SERS signal at 1578 cm^{-1} obtained from the SERS optrode with 3D porous structure is 5.9-fold greater than the intensity of the signal obtained from that decorated with only Ag NPs. For the SERS bands at 1005 and 1220 cm^{-1}, the intensities on the SERS optrode are 2.5-fold greater than the intensity of that decorated with only Ag NPs, and the intensities of the SERS signal at 1095 and 1613 cm^{-1} are 2.1-fold stronger. The Raman enhancements of different vibrational modes are different,

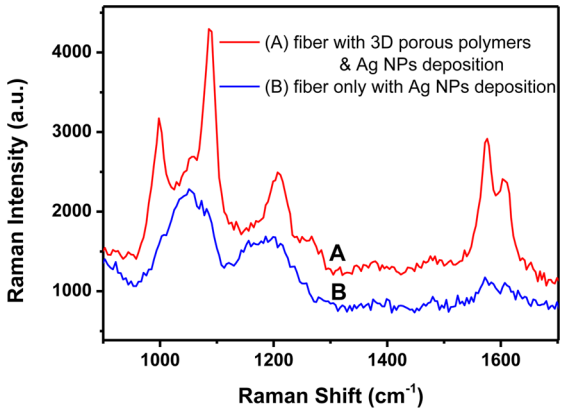

Figure 5. SERS spectra of 4-Mpy (1.0×10^{-3} M) obtained by using the SERS optrodes decorated with (A) and without (B) a porous polymer. SERS optrode A was obtained with a polymerization time of 3 min and a Ag deposition time of 5 min. SERS optrode B was achieved with a Ag deposition time of 5 min. The laser intensity for Ag deposition (532 nm) started from 33.7 mW cm^{-2} for both polymers A and B.

which is consistent with other reports.[23,35] This proves that the designed 3D porous structure supports a large surface area that allows more Ag NP locations. A high Ag NP loading and the consequent Ag aggregate response for the larger SERS contribution were found.

Figure 6 shows the concentration-dependent SERS detections of 4-Mpy and thiram with SERS optrodes. The results show that the lowest detection concentration is 1.0×10^{-8} M for both 4-Mpy and thiram with signal-to-noise (S/N) ratios of 2.6 and 3.0 (1613 cm^{-1} peak for 4-Mpy and 1375 cm^{-1} peak for thiram), respectively. The lowest detection concentration might be influenced by the absorption effect of the SERS-sensing layer (including both the polymer layer and metal nanoparticles) for the excitation photons and the SERS scattering photons. Also, the SERS radiation would be weakened upon transmission through the porous polymer layer and reached the fiber.

This SERS optrode-integrated microfluidic chip can also be used for SERS monitoring of many *in situ* reactions. We modified the SERS optrode with 4-Mpy molecules (more details in the Experimental Section). The mercapto group of 4-Mpy prefers to be linked to the surface of silver NPs, and the unoccupied N atom on pyridine is sensitive to pH because of the protonation−deprotonation reaction.[29] The pH response of 4-Mpy by SERS spectra on the SERS optrode was observed (Figure 7). It can be found that the 1578 and 1611 cm^{-1} bands, which are attributed to the pyridine ring C−C stretching mode,[29] have obviously changed with pH values in the range of 2−6.

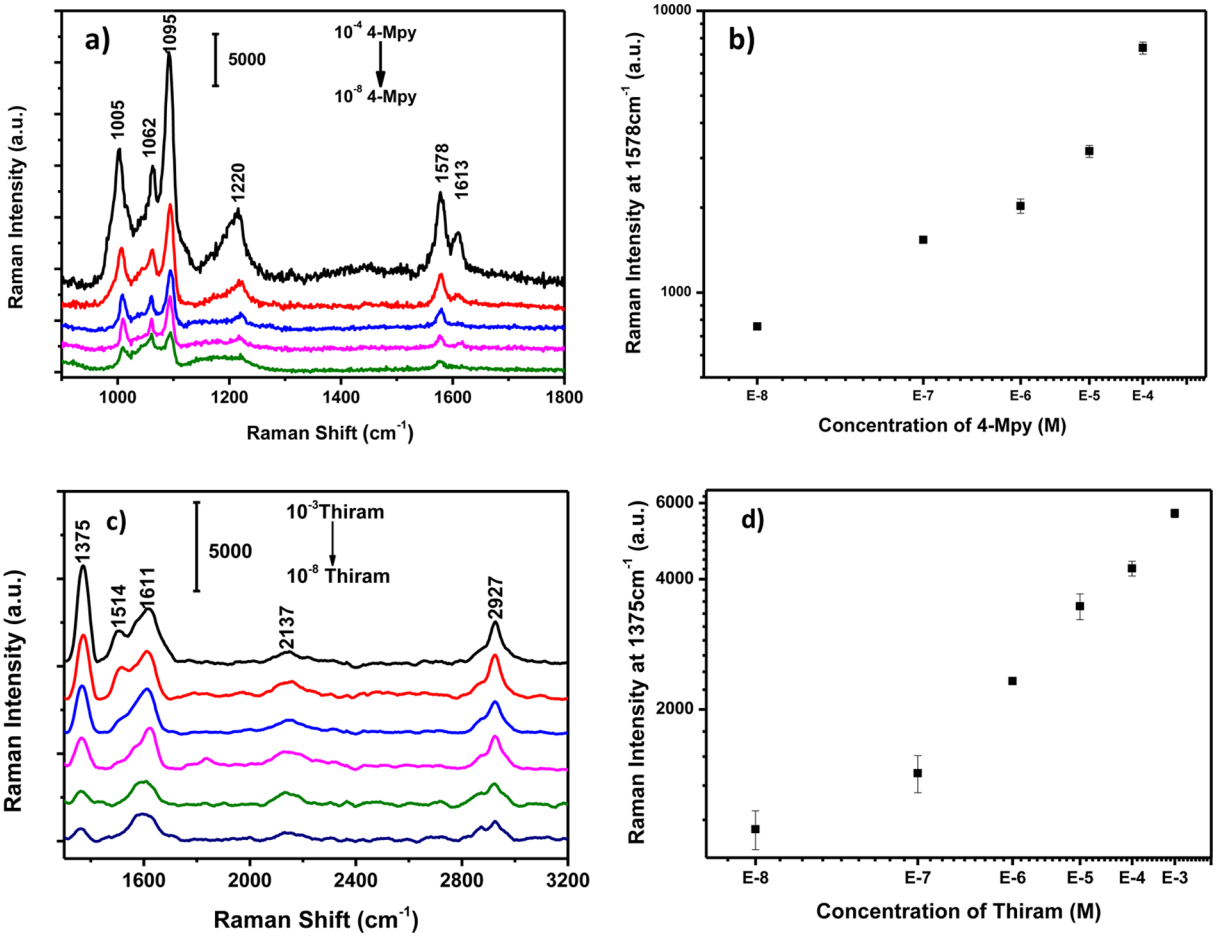

Figure 6. Concentration-dependent SERS spectra of 4-Mpy (a) and thiram (c) probed by using the SERS optrodes and the plots of SERS intensity vs 4-Mpy (b) or thiram (d) concentration. An integration time of 5 s and an accumulation time of 1 were used to record spectra shown in panel a. An integration time of 10 s and an accumulation time of 3 were used to record spectra shown in panel c.

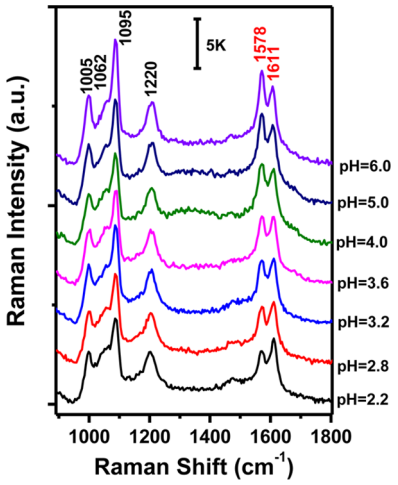

Figure 7. pH response of 4-Mpy in different buffers measured by the as-prepared SERS optrode. An integration time of 1 s and an accumulation time of 3 were used to record these spectra.

4. CONCLUSIONS

We fabricated a SERS optrode with rapid, *in situ* laser-induced polymerization and Ag deposition on an optical fiber. The whole fabrication process can be controlled by irradiation time. A large number of Ag NPs were reduced *in situ* onto the porous materials by laser illumination, ensuring the high SERS activity of this optical fiber sensor. The as-prepared SERS optrode has been combined with microfluidic chips to achieve the on-chip trace of analytes. The detection limit of this SERS optrode can reach 1.0×10^{-8} M. This SERS optrode-integrated microfluidic chip allows integration of the light path, SERS-sensing layer, and micro-sampling cell, which is promising for many applications, such as liquid analysis, reaction monitoring, bioassays, etc.

AUTHOR INFORMATION

Corresponding Author

*E-mail: xusp@jlu.edu.cn. Telephone: 86-431-85168505. Fax: 86-431-85193421.

Notes

The authors declare no competing financial interest.

ACKNOWLEDGMENTS

This work was supported by the National Instrumentation Program (NIP) of the Ministry of Science and Technology of China (2011YQ03012408), the National Natural Science Foundation of China (21373096, 21073073, and 91027010), and the Innovation Program of the State Laboratory of Supramolecular Structure and Materials.

REFERENCES

(1) Fleischmann, M.; Hendra, P.; McQuillan, A. Raman Spectra of Pyridine Adsorbed at a Silver Electrode. *Chem. Phys. Lett.* **1974**, *26*, 163−166.

(2) Chou, A.; Jaatinen, E.; Buividas, R.; Seniutinas, G.; Juodkazis, S.; Izakea, E. L.; Fredericks, P. M. SERS Substrate for Detection of Explosives. *Nanoscale* **2012**, *4*, 7419−7424.

(3) Liu, X. J.; Zong, C. H.; Ai, K. L.; He, W. H.; Lu, L. H. Engineering Natural Materials as Surface-Enhanced Raman Spectroscopy Substrates for in situ Molecular Sensing. *ACS Appl. Mater. Interfaces* **2012**, *4*, 6599−6608.

(4) Lin, W. C.; Jen, H. C.; Chen, C. L.; Hwang, D. F.; Chang, R.; Hwang, J. S.; Chiang, H. P. SERS Study of Tetrodotoxin (TTX) by Using Silver Nanoparticle Arrays. *Plasmonics* **2009**, *4*, 187−192.

(5) Gu, Y. J.; Xu, S. P.; Li, H. B.; Wang, S. Y.; Cong, M.; Lombardi, J. R.; Xu, W. Q. Waveguide-Enhanced Surface Plasmons for Ultrasensitive SERS Detection. *J. Phys. Chem. Lett.* **2013**, *4*, 3153−3157.

(6) Wolfbeis, O. S. Fiber-Optic Chemical Sensors and Biosensors. *Anal. Chem.* **2000**, *72*, 81R−89R.

(7) Wolfbeis, O. S. Fiber-Optic Chemical Sensors and Biosensors. *Anal. Chem.* **2002**, *74*, 2663−2678.

(8) Yamamoto, Y. S.; Oshima, Y.; Shinzawa, H.; Katagiri, T.; Matsuura, Y.; Ozaki, Y.; Sato, H. Subsurface Sensing of Biomedical Tissues Using a Miniaturized Raman Probe: Study of Thin-Layered Model Samples. *Anal. Chim. Acta* **2008**, *619*, 8−13.

(9) Fan, M. K.; Wang, P. H.; Escobedo, C.; Sintond, D.; Brolo, A. G. Surface-Enhanced Raman Scattering (SERS) Optrodes for Multiplexed On-Chip Sensing of Nile Blue A and Oxazine 720. *Lab Chip* **2012**, *12*, 1554−1560.

(10) Viets, C.; Hill, W. Comparison of Fibre-Optic SERS Sensors with Differently Prepared Tips. *Sens. Actuators, B* **1998**, *51*, 92−99.

(11) Amezcua-Correa, A.; Yang, J. X.; Finlayson, C. E.; Peacock, A. C.; Hayes, J. R.; Sazio, P. J. A.; Baumberg, J. J.; Howdle, S. M. Surface-Enhanced Raman Scattering Using Microstructured Optical Fiber Substrates. *Adv. Funct. Mater.* **2007**, *17*, 2024−2030.

(12) Lucotti, A.; Pesapane, A.; Zerbi, G. Use of a Geometry Optimized Fiber-Optic Surface-Enhanced Raman Scattering Sensor in Trace Detection. *Appl. Spectrosc.* **2007**, *61*, 260−268.

(13) Lucotti, A.; Zerbi, G. Fiber-optic SERS Sensor with Optimized Geometry. *Sens. Actuators, B* **2007**, *121*, 356−364.

(14) Xu, W. Q.; Xu, S. P.; Hu, B.; Wang, K. X.; Zhao, B.; Xie, Y. T.; Fan, Y. G. Studies on the SERS-Active Optic Fiber Probe. *Gaodeng Xuexiao Huaxue Xuebao* **2004**, *25*, 144−147.

(15) Jia, S. J.; Xu, S. P.; Zheng, X. L.; Zhao, B.; Xu, W. Q. Preparation of SERS Optical Fiber Sensor Via Laser-Induced Deposition of Ag Film on the Surface of Fiber Tip. *Gaodeng Xuexiao Huaxue Xuebao* **2006**, *27*, 523−526.

(16) Zheng, X. L.; Guo, D. W.; Shao, Y. L.; Jia, S. J.; Xu, S. P.; Zhao, B.; Xu, W. Q.; Corredor, C.; Lombardi, J. R. Photochemical Modification of an Optical Fiber Tip With a Silver Nanoparticle Film: A SERS Chemical Sensor. *Langmuir* **2008**, *24*, 4394−4398.

(17) Ming, S. L.; Chang, X. Y. Laser-Induced Silver Nanoparticles Deposited on Optical Fiber Core for Surface-Enhanced Raman Scattering. *Chin. Phys. Lett.* **2010**, *27*, 044202.

(18) Liu, T.; Xiao, X. X.; Yang, C. X. Surfactantless Photochemical Deposition of Gold Nanoparticles on an Optical Fiber Core for Surface-Enhanced Raman Scattering. *Langmuir* **2011**, *27*, 4623−4626.

(19) Banholzer, M. J.; Millstone, J. E.; Qin, L.; Mirkin, C. A. Rationally Designed Nanostructures for Surface-Enhanced Raman Spectroscopy. *Chem. Soc. Rev.* **2008**, *37*, 885−897.

(20) Baker, G. A.; Moore, D. S. Progress in Plasmonic Engineering of Surface-Enhanced Raman-Scattering Substrates Toward Ultra-Trace Analysis. *Anal. Bioanal. Chem.* **2005**, *382*, 1751−1770.

(21) Xu, H. X.; Aizpurua, J.; Käll, M.; Apell, P. Electromagnetic Contributions to Single-Molecule Sensitivity in Surface-Enhanced Raman Scattering. *Phys. Rev. E* **2000**, *62*, 4318.

(22) Michaels, A. M.; Nirmal, M.; Brus, L. Surface Enhanced Raman Spectroscopy of Individual Rhodamine 6G Molecules on Large Ag Nanocrystals. *J. Am. Chem. Soc.* **1999**, *121*, 9932−9939.

(23) Tseng, M. L.; Chang, C. M.; Cheng, B. H.; Wu, P. C.; Chung, K. S.; Hsiao, M. K.; Huang, H. W.; Huang, D. W.; Chiang, H. P.; Leung, P. T.; Tsai, D. P. Multi-level Surface Enhanced Raman Scattering Using AgO_x Thin Film. *Opt. Express* **2013**, *21*, 24460−24467.

(24) Cho, W. J.; Kim, Y.; Kim, J. K. Ultrahigh-Density Array of Silver Nanoclusters for SERS Substrate with High Sensitivity and Excellent Reproducibility. *ACS Nano* **2012**, *6*, 249−255.

(25) Viklund, C.; Pontén, E.; Glad, B.; Irgum, K.; Hörstedt, P.; Svec, F. "Molded" Macroporous Poly(glycidyl methacrylate-co-trimethylolpropane trimethacrylate) Materials with Fine Controlled Porous

Properties: Preparation of Monoliths Using Photoinitiated Polymerization. *Chem. Mater.* **1997**, *9*, 463−471.
(26) Walsh, Z.; Abele, S.; Lawless, B.; Heger, D.; Klán, P.; Breadmore, M. C.; Paull, B.; Macka, M. Photoinitiated Polymerisation of Monolithic Stationary Phases in Polyimide Coated Capillaries Using Visible Region LEDs. *Chem. Commun.* **2008**, 6504−6506.
(27) Lee, D.; Svec, F.; Fréchet, J. M. Photopolymerized Monolithic Capillary Columns for Rapid Micro High-Performance Liquid Chromatographic Separation of Proteins. *J. Chromatogr., A* **2004**, *1051*, 53−60.
(28) Svec, F. Less Common Applications of Monoliths: I. Microscale Protein Mapping with Proteolytic Enzymes Immobilized on Monolithic Supports. *Electrophoresis* **2006**, *27*, 947−961.
(29) Hu, J. W.; Zhao, B.; Xu, W. Q.; Li, B. F.; Fan, Y. G. Surface-Enhanced Raman Spectroscopy Study on the Structure Changes of 4-Mercaptopyridine Adsorbed on Silver Substrates and Silver Colloids. *Spectrochim. Acta, Part A* **2002**, *58*, 2827−2834.
(30) Cao, Q.; Xu, Y.; Liu, F.; Svec, F.; Fréchet, J. M. Polymer Monoliths with Exchangeable Chemistries: Use of Gold Nanoparticles as Intermediate Ligands for Capillary Columns with Varying Surface Functionalities. *Anal. Chem.* **2010**, *82*, 7416−7421.
(31) Lv, Y.; Alejandro, F. M.; Fréchet, J. M.; Svec, F. Preparation of Porous Polymer Monoliths Featuring Enhanced Surface Coverage with Gold Nanoparticles. *J. Chromatogr., A* **2012**, *1261*, 121−128.
(32) Svec, F. Porous Polymer Monoliths: Amazingly Wide Variety of Techniques Enabling Their Preparation. *J. Chromatogr., A* **2010**, *1217*, 902−924.
(33) Liu, J.; White, I.; DeVoe, D. L. Nanoparticle-Functionalized Porous Polymer Monolith Detection Eelements for Surface-Enhanced Raman Scattering. *Anal. Chem.* **2011**, *83*, 2119−2124.
(34) Li, Q. Q.; Du, Y. P.; Tang, H. R.; Wang, X.; Chen, G. P.; Iqbal, J.; Wang, W. M.; Zhang, W. B. Ultra Sensitive Surface-Enhanced Raman Scattering Detection Based on Monolithic Column as a New Type Substrate. *J. Raman Spectrosc.* **2012**, *43*, 1392−1396.
(35) Ling, X.; Xie, L. M.; Fang, Y.; Xu, H.; Zhang, H. L.; Kong, J.; Dresselhaus, M. S.; Zhang, J.; Liu, Z. F. Can Graphene be used as a Substrate for Raman Enhancement? *Nano Lett.* **2010**, *10*, 553−561.